



Characterizing the temperature and precipitation covariability over Canada

Harsimrenjit Singh¹ · Farshad Jalili Pirani¹ · Mohammad Reza Najafi¹

Received: 19 June 2019 / Accepted: 25 November 2019 / Published online: 14 December 2019
© Springer-Verlag GmbH Austria, part of Springer Nature 2019

Abstract

Changes in the regional characteristics of temperature and precipitation can intensify the occurrence and severity of extreme events such as rain-on-snow-induced flooding, droughts and wildfires. Analyzing these climate variables in isolation without considering their interdependencies might result in severe underestimation of their combined effects. In addition, the assumption of linearity between temperature and precipitation does not represent the real physical processes that govern these climate variables. In this study, copula functions are used to describe the joint behaviour of temperature and precipitation across 15 ecozones of Canada at multiple temporal scales. The Clausius-Clapeyron (CC) relation is investigated using daily records to quantify changes in extreme precipitation with temperature increases. In addition, using historical records, dating back to 1910s, temporal changes in the dependence structure across southern Canada are analyzed using a non-stationary framework. Results show clear signs of accelerated warming and wetting over northern Canada while strong evidence of hot and dry conditions is found in the Prairie provinces. Analyses over seasonal and monthly scales indicate increases in warm-wet and hot-dry conditions in winter and summer, respectively. Non-stationary analyses reveal shifts towards warm and wet climate conditions for the majority of southern Canada. Considerable deviations from the theoretical CC scaling rate of 6.8% is observed for extreme precipitation over parts of Canada with super-CC scaling rates observed in northern Canada and sub-CC scaling rates in the majority of southern Canada.

1 Introduction

The recently published Canada's Changing Climate Report (CCCR 2019) states that the global mean surface temperature has increased by 0.6 °C in 1986–2005 compared with the pre-industrial period (1850–1900). Future temperature is projected to increase by 1 °C under the low emission scenario and 3.7 °C under the high emission scenario by the end of the twenty-first century with respect to the reference period of 1986–2005 (Bush and Lemmen 2019). Vincent et al. (2015) reported an overall temperature increase of 1.7 °C over Canada from 1948 to 2012 with the largest increase of 3.3 °C in winter and the lowest of 1.4 °C in summer. They

reported a 19% increase in precipitation during the same period. Vincent et al. (2018) reported an increase in the frequency of summer days and hot days, and increases in rainfall accompanied by decreases in snowfall over southern Canada. Changes in temperature and precipitation have resulted in reduced snowpack and Arctic sea-ice (Najafi et al. 2016; Najafi et al. 2017b; Min et al. 2008), changes in surface water availability (Najafi et al. 2017a), increased evapotranspiration, increased depth and extent of permafrost thaw, more frequent droughts and flooding, among others (Blankinship and Hart 2012; Warren and Lemen 2014).

Understanding the interdependencies between temperature and precipitation can improve the prediction of extreme events such as floods and droughts and help better project the impacts of climate change. Information obtained from an isolated study of these climate variables fails to capture the conditional effects of other drivers that are caused by their mutual interactions. This can result in a misrepresentation of the joint physical processes and the possible underestimation of hydrological hazards and risks (Favre et al. 2004; Hao and Singh 2016). Multivariate analysis approaches based on bivariate normal distributions or other multivariate extensions of student's *t* and Fischer's *F*

Electronic supplementary material The online version of this article (<https://doi.org/10.1007/s00704-019-03062-w>) contains supplementary material, which is available to authorized users.

✉ Mohammad Reza Najafi
mnajafi7@uwo.ca

¹ Department of Civil and Environmental Engineering, Western University, London, ON, Canada

distributions can be used to characterize the dependencies between temperature and precipitation (Anderson 1962; Johnson and Wichern 2002). However, these approaches are marred by drawbacks, such as the inability of a bivariate Gaussian distribution to capture the dependence of extremes (i.e. tails of the distribution). Moreover, they require the marginal distributions to belong to the same family as the bivariate distribution and offer no solution for cases beyond the bivariate dimension (Favre et al. 2004). Such homogeneity assumptions across distributions do not always hold.

In this study, we use copula functions (Sklar 1959), which address the aforementioned restraints. Copulas are flexible family of functions that can bind a multivariate distribution with the constituent univariate marginal distributions irrespective of the homogeneities in the families of distributions (Frees and Valdez 1998). Copulas have been an integral component of financial modelling, and their applications in hydrology have grown considerably in recent years as they can represent the complex non-linear dependence structures between hydroclimatic variables (Favre et al. 2004; Laux et al. 2011; Lazoglou and Anagnostopoulou 2019). Several studies have been conducted to model droughts in a multivariate framework using copulas (Shiau 2006; Wong et al. 2009). Schoelzel and Friederichs (2008) reported the advantages of copulas over other multivariate methods such as mixture models using ground-based temperature and precipitation observations in Berlin. Beniston (2009) studied the trends of higher and lower quantiles of precipitation and temperature over nine locations in Europe. Using regional climate models, they found a decrease in cold/dry conditions and an increase in wet/warm conditions from 1900 to 2100. Cong and Brady (2012) analyzed the relations between April precipitation and temperature in Sweden from 1960 to 2010 using five copula families. Rana et al. (2017) studied the joint distribution of daily precipitation and temperature using an ensemble of 10 global climate models over the Columbia River Basin in the USA. They reported that temperature and precipitation have a negative relationship in the dry season; whereas in wet seasons, precipitation is mostly independent of temperature changes. Their analyses showed a significant positive trend for both temperature and precipitation in the future. Only a limited number of studies, mostly restricted to regional scales, have explored the joint variability of temperature and precipitation in Canada. Asong et al. (2016) used Generalized Linear Models to study temperature and precipitation over the Canadian Prairies. Gennaretti et al. (2015) and Guerfi et al. (2015) used copulas to model temperature and precipitation over the Canadian Arctic coastal zones and southern Quebec, respectively. Tencer et al. (2014) conducted a pan-Canadian study of temperature and precipitation extremes. They analyzed the joint daily occurrence of extreme precipitation and extreme temperature (higher and lower quantiles) at 293 sites across Canada using

non-parametric methods. They found a strong positive relationship between high temperature and precipitation in eastern and southwestern coastal areas in autumn and winter and a strong relationship between precipitation and low temperature in spring and summer. Other studies have analyzed the relationship between temperature and precipitation globally but their analyses have been restricted to exploring the linear associations between the two variables (Déry and Wood 2005; Trenberth and Shea 2005). These studies have reported strong positive correlations between the two variables at higher latitudes, especially in winter; however, they also acknowledge the presence of non-linearity in the dependence structure. Another approach to study the association between precipitation and temperature is the theoretical Clausius-Clapeyron (CC) relation, which states that the water holding capacity of the air rises by about 7% for every 1 K increase in air temperature (Pall et al. 2007). Allen et al. (2010) reported that whereas the global mean precipitation has a scaling rate of about 3.4%, extreme precipitation follows the CC relation more closely.

Previous studies have reported trends in both temperature and precipitation (Vincent et al. 2015; Zhang et al. 2000) which can result in temporal changes in the dependence structure between these climate variables. While characterizing this trend is critical for hazard risk assessments and the design of infrastructure, most studies have focused on temporal variations of the individual variables in isolation assuming that their covariabilities will remain unchanged. Only a few studies have considered non-stationarity in a bivariate framework (Hao and Singh 2016).

In this study, we use copulas to characterize the joint behaviour of temperature and precipitation in 15 ecozones across Canada at multiple time scales. In addition, CC scaling curves are generated to characterize extreme precipitation response to temperature changes within each zone. Next, we evaluate the non-stationary joint behaviour of temperature and precipitation following the approach proposed by Bender et al. (2014). The study aims to answer the following questions:

- Do temperature and precipitation exhibit significant non-linear relationships over Canada?
- How does precipitation respond to temperature changes over different regions in Canada?
- Is the dependence structure between temperature and precipitation changing over time?

The remainder of the paper is organized as follows: Section 2 describes the study area and observed datasets. Section 3 discusses the methodology including the precipitation and temperature covariability scenarios, the non-stationary approach, copula and the corresponding model selection criteria. Results and conclusions are presented in Section 4 and Section 5, respectively.

2 Study area and data

Canada is the second-largest country in the world, covering an area of over 9.9 million km². It is surrounded by the Pacific, Atlantic and Arctic Oceans on the west, east and north, respectively, and the USA on the south. The extensive variety of geographical features, presence of the oceans, the Great Lakes in southern parts of Ontario and mountain ranges in the west generate a diverse array of climatic conditions throughout the country. Areas in the north experience polar and sub-Arctic climate conditions, eastern provinces have a temperate climate and southwestern regions experience a hot and humid summer continental climate (Peel et al. 2007).

The study area is divided into 15 ecozones (Fig. 1), which were characterized by Wiken (1986) as a way to define, “on a subcontinental scale, the broad mosaics formed by the interaction of macroscale climate, human activity, vegetation, soils, geological, and physiographic features of the country” and were used in the first State of the Environment Report for Canada in 1986 (Bird and Rapport 1986).

Adjusted and Homogenized Canadian Climate Data (AHCCD) at a daily time scale is used in this study. AHCCD is a corrected version of the historical station records created by removing various non-climatic inconsistencies

such as instrument changes, station relocation, wind undercatch, evaporation and wetting losses for precipitation (Mekis and Vincent 2011) and corrections to temperature for temporal gaps, inhomogeneities and a nation-wide change for time observation (Vincent et al. 2012). Temperature and precipitation records from 107 stations with at least 80% data availability from 1950 to 2010 are considered for the analyses. This time period is selected to provide a balance between the spatial spread of the stations and the length of the dataset. Zones 1 and 11 (the Arctic Cordillera and Taiga Cordillera, respectively) are excluded from the analyses because of the limited data availability (> 50% missing data). An exception is made for Zone 4 (Taiga Plains) where two stations with 78% available data are selected to avoid excluding this zone. To analyze the non-stationary dependence structure between temperature and precipitation, we use 66 AHCCD stations (a subset of the already selected 107) with long historical records (1910–2017) and over 80% data availability (Fig. 1). The end period of the analysis was extended to 2017 in this case because it was desirable to include the longest possible timespan available. Consequently, non-stationary analyses are conducted over eight zones (Zones 6–9 and Zones 12–14). Table 1 shows the mean summer and winter temperatures, along with the mean annual precipitation in each ecozone (Lands Directorate 1986).

Fig. 1 Ecozones of Canada as defined by Wiken (1986) and the location of the selected Adjusted and Homogenized Canadian Climate Data (AHCCD) Stations. Total of 107 stations are used in the study. A further subset of 66 stations from the selected 107 are used for the long-term non-stationary analysis

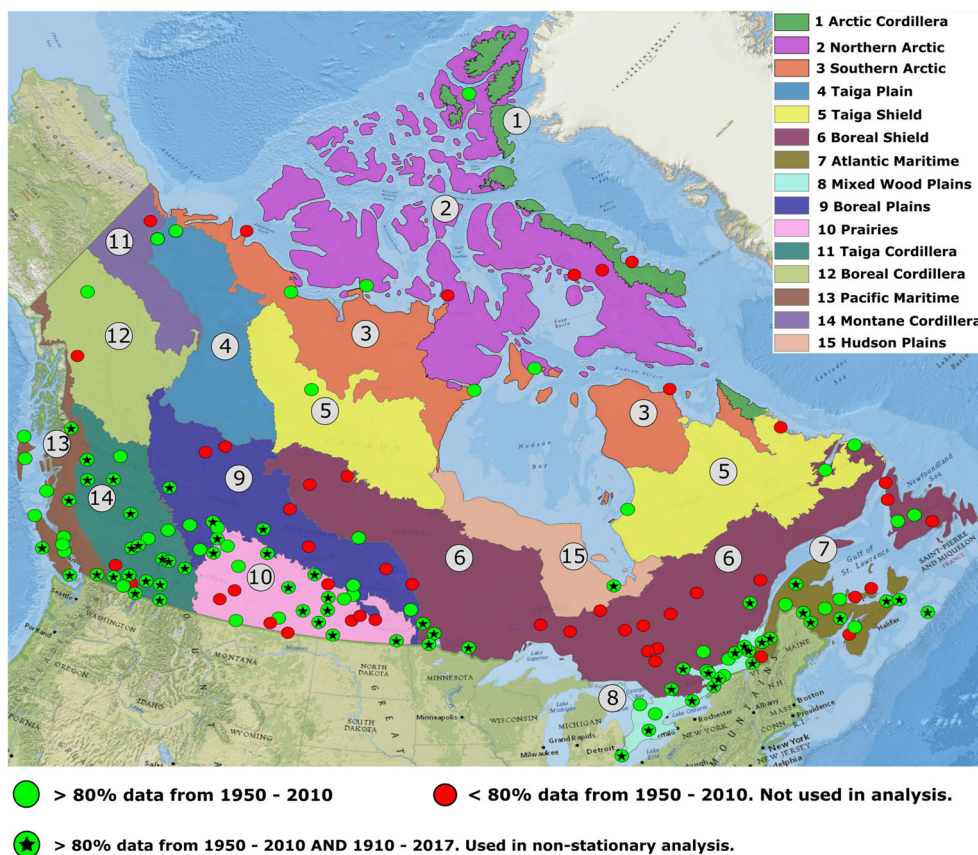


Table 1 Climatology of terrestrial ecozones of Canada

Ecozone	Mean winter temperature (°C)	Mean summer temperature (°C)	Mean annual precipitation (mm year ⁻¹)
1 – Arctic Cordillera	– 35 to – 25	5	200 to 300
2 – Northern Arctic	– 35 to – 30	5 to 10	100 to 200
3 – Southern Arctic	– 30	10	200 to 400
4 – Taiga Plains	– 35 to – 22.5	10 to 15	200 to 400
5 – Taiga Shield	– 27.5 to 17.5	7.5 to 17.5	175 to 200
6 – Boreal Shield	– 20 to – 10	15 to 18	400 to 1000
7 – Atlantic Maritime	– 10 to – 2.5	18	1000 to 1425
8 – Mixedwood Plains	– 12 to – 3	18 to 22	720 to 1000
9 – Boreal Plains	– 22.5 to – 17.5	12.5 to 17.5	400 to 500
10 – Prairies	– 25 to – 22.5	15 to 17.5	400
11 – Taiga Cordillera	– 30 to – 25	12 to 15	300
12 – Boreal Cordillera	– 27 to – 15	12 to 15	1000 to 1500
13 – Pacific Maritime	4 to 6	12 to 18	600 to 3000
14 – Montane Cordillera	– 17.5 to 7.5	13 to 18	500 to 1200
15 – Hudson Plains	– 19	12 to 16	400 to 700

3 Methods

3.1 Copulas

Copulas, first introduced by Sklar (1959), allow for the characterization of the dependence structure between two (or more) variables independent from their marginal distributions (Genest and Favre 2007; Schmidt 2007). Sklar's theorem states that given two continuous random variables X and Y , the joint Cumulative Distribution Function (CDF) $H(X, Y)$ can be written as:

$$H(X, Y) = C[F(X), G(Y)] \quad (1)$$

where $F(X)$ and $G(Y)$ are the marginal distributions of X and Y , respectively, and C is the copula function built over uniform marginals, which are the quantile transformations of X and Y . The determination of the joint CDF $H(X, Y)$ then becomes a two-step process of finding the dependence structure C and the marginal distributions of X and Y (Zhang and Singh 2006). This concept is extendable to multivariate scenarios (Nelsen 2006).

In this study, multiple families of copulas are used, each having their own unique set of properties, which allows for a wide range of models to choose from when identifying the bivariate structure (Favre et al. 2004; Salvadori and De Michele 2004). They include the elliptical, Archimedean and extreme value copulas, and their rotated versions (90, 180 or survival, and 270). All types of copulas used in this study are listed in Table 2 along with their corresponding symbols, which are used to reference the respective copula for the remainder of the paper.

A brief description of some widely used copulas is provided in the Appendix. The two-parameter families of copulas, such as BB1, provide the flexibility of modelling asymmetric upper and lower tail dependencies. Joe (2014) and Nelsen (2006) provide an extensive explanation of all classes of copulas and their characteristics.

Given the high intra-annual variations of temperature and precipitation, it is important to understand their dependence structure at different temporal scales for hazard risk assessments. In this study, analyses are performed at the annual, seasonal and monthly scales based on daily records of temperature and precipitation spatially averaged over the ecozones by taking the arithmetic mean of all stations lying within each zone. In each scenario, accumulated precipitation (millimetres) and mean temperature (°C) are calculated at the corresponding time scale:

$$P_i^* = \sum_{d=1}^n P_d, \text{ where } P_d = \frac{\sum P_{1\dots K}}{K} \quad (2)$$

$$T_i^* = \sum_{d=1}^n \frac{T_d}{n}, \text{ where } T_d = \frac{\sum T_{1\dots K}}{K} \quad (3)$$

where ($d = 1, \dots, n$) denotes the number of days in each year, season or month of the year ($i = 1950, 1951, \dots, 2010$). P_d and T_d are spatial averages of temperature and precipitation across K stations within each ecozone. The seasonal analysis is conducted over winter (DJF), spring (MAM), summer (JJA) and fall (SON). Analyses at daily time scales are not shown because of the weak correlations between temperature and precipitation due to the large noise in the data at this temporal resolution. The same procedure is repeated for standardized anomalies of temperature and precipitation, which shows negligible changes in the rank correlation. Therefore, values in

Table 2 The list of copulas used in this study

Symbol	Copula name	Symbol	Copula name
C0	Independent	C20	Rotated Joe 90 degrees
C1	t	C21	Rotated BB1 90 degrees
C2	Gaussian	C22	Rotated BB6 90 degrees
C3	Clayton	C23	Rotated BB7 90 degrees
C4	Gumbel	C24	Rotated BB8 90 degrees
C5	Frank	C25	Rotated Clayton 270 degrees
C6	Joe	C26	Rotated Gumbel 270 degrees
C7	BB1	C27	Rotated Joe 270 degrees
C8	BB6	C28	Rotated BB1 270 degrees
C9	BB7	C29	Rotated BB6 270 degrees
C10	BB8	C30	Rotated BB7 270 degrees
C11	Survival Clayton	C31	Rotated BB8 270 degrees
C12	Survival Gumbel	C32	Tawn type 1
C13	Survival Joe	C33	Rotated Tawn type 1180 degrees
C14	Survival BB1	C34	Rotated Tawn type 1 90 degrees
C15	Survival BB6	C35	Rotated Tawn type 1270 degrees
C16	Survival BB7	C36	Tawn type 2
C17	Survival BB8	C37	Rotated Tawn type 2180 degrees
C18	Rotated Clayton 90 degrees	C38	Rotated Tawn type 2 90 degrees
C19	Rotated Gumbel 90 degrees	C39	Rotated Tawn type 2270 degrees

their original scales are used in the analyses because they provide more realistic interpretations of the regional changes.

3.2 Model selection criteria

Selection of the most suitable copula is based on the corrected version of the Akaike Information Criterion (AIC_c) (Akaike 1974), which is defined as:

$$AIC_c = -2 \sum_{i=1}^N \ln[C(u_{i,1}, v_{i,2}|\theta)] + 2k + \frac{2k^2 + 2k}{n-k-1} \quad (4)$$

where k is the number of parameters of the copula ($k=1$ for one-parameter and $k=2$ for two-parameter families) and n is the sample size (Schepsmeier et al. 2018). The first term of the right-hand side of Eq. (4) is the likelihood function, the second is the penalty for model complexity and the last expression is the small-sample correction. AIC_c is used as a small-sample corrected version of AIC when the sample size to model parameter ratio (n/k) is under 40. It converges to AIC as the sample size gets larger (Anderson and Burnham 2004). The copula model with the lowest AIC_c is selected as it minimizes the information loss between the unknown true copula and the selected model (Anderson and Burnham 2004). The marginal distributions of temperature and precipitation are selected from a pool of candidate distributions using AIC_c . For precipitation, the candidate distributions are

Gamma, Weibull, Exponential and Log-Normal, whereas normal distribution is selected to model temperature.

The selection criteria based on the information theory would only provide a relative score of the models considered raising the question “What if all the models are wrong?” since a comparison between all “wrong” models would still provide one model with the best relative score (Burnham et al. 2011). Therefore, in this study, additional goodness-of-fit test proposed by Genest et al. (2006) is used to evaluate the selected models. The goodness-of-fit test is based on calculating two variants of the Cramér–von Mises statistic (Genest and Favre 2007).

$$S_n = \int_0^1 |K_n(t)|^2 K_{\theta_n}(t) dt \quad (5)$$

$$T_n = \sup_{0 \leq t \leq 1} |K_n(t)| \quad 0 \leq t \leq 1 \quad (6)$$

where $K_n(t) = \sqrt{n}\{K_n(t) - K_{\theta_n}(t)\}$. Here, K_n refers to the empirical distribution of the data and K_{θ_n} refers to the theoretical distribution of samples taken from the selected copula. This method is an improvement over the previous works of Genest and Rivest (1993) and Wang and Wells (2000). The enhancements over previous approaches include the extension of the goodness-of-fit test beyond the Archimedean family of copulas and the estimation of p values of the statistic. Genest et al. (2006) reported that the comparison of raw values of the statistics S_n and T_n may be inappropriate in model selection in

some cases. To rectify this drawback, they proposed a bootstrapping procedure to estimate p values under the null hypothesis, $H_0 : C_\theta \in C_{\theta_n}$ where C_θ is the underlying empirical copula and C_{θ_n} is a parametric family of copulas under consideration. The procedure is based on identifying the asymptotic null distribution from which the empirical statistics S_n and T_n are obtained (Genest and Rémillard 2008). Following similar works by Henze (1996) and Stute et al. (1993), they proposed generating n independent observations from the parametric family C_{θ_n} and calculating the statistics S_n^* and T_n^* for the sample. The process is repeated for a large number of times to obtain distributions of the statistics following which p values are estimated according to the following equation:

$$\frac{1}{N} \sum_{k=1}^N 1(S_{n,k}^* > S_n) \quad (7)$$

for every $k \in \{1 \dots N\}$, where N is the number of times the procedure is repeated. In this study, each copula is evaluated at $N = 1000$ iterations.

3.3 Non-stationary dependence structure

Non-stationary analyses of the dependence structure require long records of climate variables. Considering data availability, the time period of 1910–2017 is selected to analyze the non-stationary covariability between temperature and precipitation over 66 stations in eight ecozones. First, a non-parametric Mann-Kendall trend test is used to evaluate the trends of both temperature and precipitation at each zone. Since the presence of serial correlation can increase the chances of rejecting a no-trend null hypothesis (Zwiers and Von Storch 1995), the series is pre-whitened before applying the trend test when significant serial correlations exist (at the 95% confidence level). If a significant trend is found in either one of the series, moving-window dependency analysis is conducted following Bender et al. (2014) by considering a window size of 50 years with 1-year increments. A stationary copula model is fitted to data in each window using methods described previously. This approach provides a fine balance between sufficiently long records within each window for a reasonable marginal and copula fitting procedure and total number of windows to detect a change in trend.

3.4 Clausius-Clapeyron scaling relation

The CC scaling coefficient is determined for each ecozone similar to Hardwick Jones et al. (2010). The daily temperature is divided into 2 °C bins (with 1 °C overlap for smoothing). Precipitation over the full 61-year period (1950–2010) is assigned to each bin and the 95th, 99th and 99.9th quantiles within each bin are calculated as representatives of extreme precipitation for the specific average bin temperature. The

following equation is used to relate extreme precipitation to temperature changes:

$$P_2 = P_1(1 + a)^{\Delta T} \quad (8)$$

where P_1 and P_2 are extreme precipitation rates in mm day⁻¹ (95th, 99th and 99.9th quantiles) at temperatures T_1 and T_2 (°C), respectively. ΔT is the change in temperature ($T_2 - T_1$) and a is the scaling coefficient, which is theoretically equal to 6.8% °C⁻¹ at 25 °C. To determine this coefficient for each ecozone, a linear regression model is fitted to temperature and logarithm of extreme precipitation as per Eq. (8).

4 Results and discussion

It is imperative to state that the aim of this study is not to establish a direct one-to-one causal relationship between precipitation and temperature. As stated by Isaac and Stuart (1992) “temperature-precipitation relationship does not provide strong evidence for any cause and effect. Certainly, stability indices, pressure, upper airflow, and temperature-dew point spreads are more directly related to precipitation-formation mechanisms.” However, temperature is one of the most well-recorded and well-studied climate variables, whereas our capability to predict precipitation is limited due to the complex interactions between multiple factors. Therefore, characterizing the covariability between precipitation and temperature can improve our understanding of precipitation behaviour as well as the joint impact of the two variables.

4.1 The dependency of total annual precipitation on mean temperature

The annual temperature series are normally distributed, whereas precipitation is described by Gamma and Weibull distributions in all ecozones. Table 3 shows the average rank correlation between temperature and precipitation in all zones at the annual time scale. Statistically significant Kendall’s rank coefficient values at a significance level of 5% are found in seven zones. Except Zone 9 and Zone 10 (Boreal Plains and Prairies) that exhibit negative correlations, the temperature is positively correlated with precipitation in other parts of Canada. The strongest positive relationship is observed around Hudson Bay, specifically in southern Arctic and Taiga shield ecozones with $\tau = 0.28$ and 0.26, respectively. Relatively stronger positive correlations in northern zones follow the trends reported by Bush and Lemmen (2019) and Environment Canada (2014) of northern Canada getting warmer and wetter at an increasingly higher rate compared with the global average. Copulas for each zone were selected according to the AIC_c model selection criteria and the goodness-of-fit was evaluated as described in Section 3.1.

Table 3 Kendall's rank correlation coefficients for 15 ecozones at an annual timescale. The *p* values marked with asterisks show statistically significant correlations at a 5% significance level

Zone	Kendall's rank correlation coefficient	<i>p</i> value (5% Significance Level)	Number of stations
1 – Arctic Cordillera	NA	NA	NA
2 – Northern Arctic	0.11	0.23	2
3 – Southern Arctic	0.28	0.00*	3
4 – Taiga Plains	0.19	0.02*	2
5 – Taiga Shield	0.26	0.00*	3
6 – Boreal Shield	0.09	0.47	14
7 – Atlantic Maritime	0.22	0.01*	13
8 – Mixedwood Plains	0.05	0.88	12
9 – Boreal Plains	−0.18	0.04*	9
10 – Prairies	−0.23	0.00*	16
11 – Taiga Cordillera	NA	NA	NA
12 – Boreal Cordillera	0.15	0.08	1
13 – Pacific Maritime	0.09	0.71	12
14 – Montane Cordillera	0.06	0.79	19
15 – Hudson Plains	0.17	0.05*	1

The dependence structure of the two variables is shown for the southern Arctic (based on the Joe copula) and the Prairies (based on the R270 Clayton copula) with contrasting joint behaviour. The model shows upper tail dependency in the southern Arctic indicating that higher values of temperature tend to correlate with higher precipitation values. The copula density shows a peak at a temperature near $-16\text{ }^{\circ}\text{C}$ and precipitation $\sim 350\text{ mm year}^{-1}$. The stations in this zone are not ideally representative of the climate regime of the entire ecozone as they are located on the northern edge resulting in a slight cold bias. Bintanja and Selten (2014) discussed how precipitation in the Arctic region is driven primarily by “local surface evaporation” thus establishing the direct impact of the Arctic warming on precipitation amounts. Positive correlations and dependency in the upper tails (extremes) between temperature and precipitation suggest that rising temperature could intensify precipitation due to increased evaporation. For the Prairies, the copula peak is observed at a temperature of $3\text{ }^{\circ}\text{C}$ and around 500 mm year^{-1} precipitation. There is the presence of higher dependency for low temperatures and high precipitation, which diminishes as the temperature gets warmer (Fig. 2).

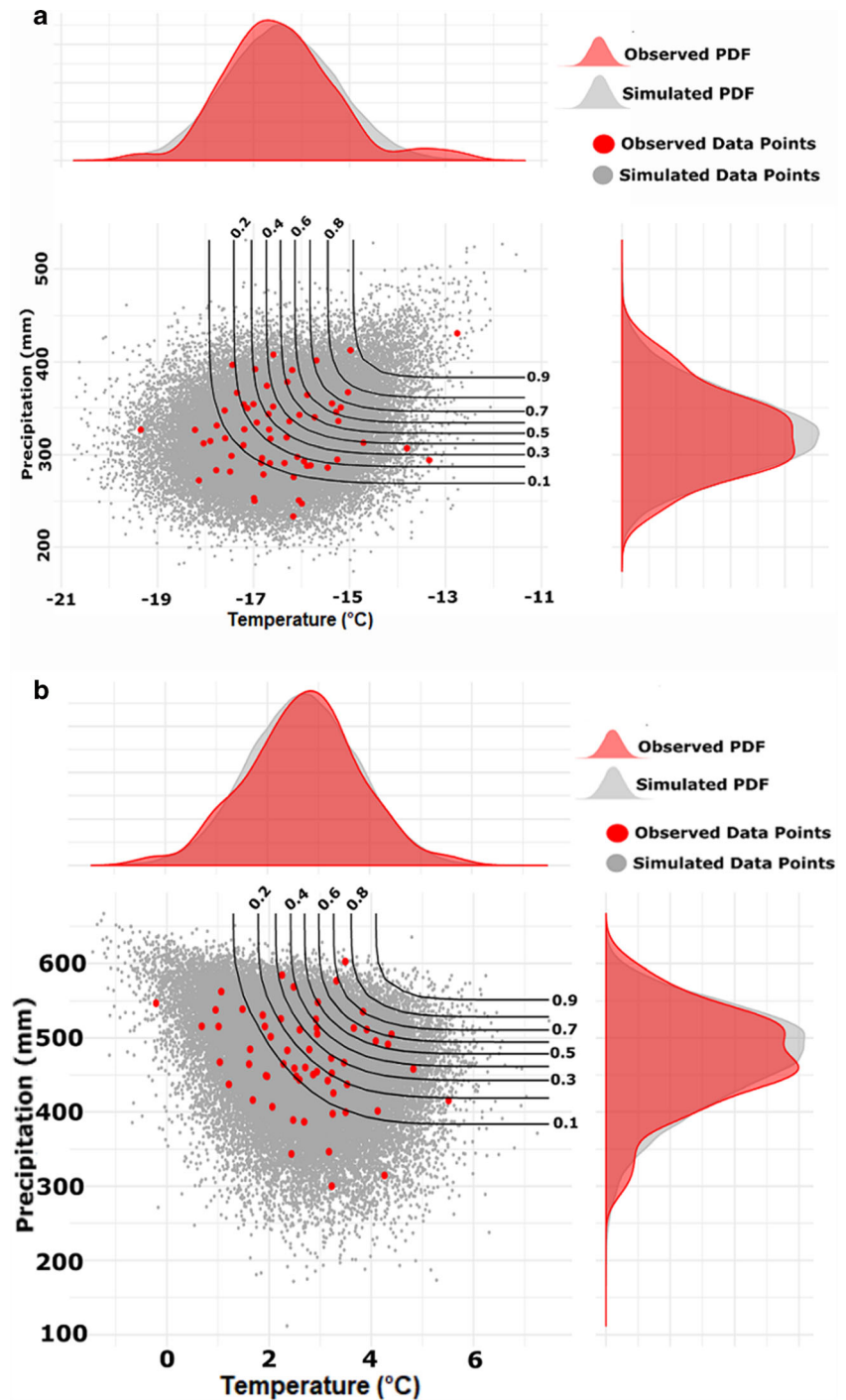
4.2 Seasonal dependency

The northern and southern Arctic zones are the only two zones that maintain a positive correlation between temperature and precipitation throughout the four seasons indicating that the northern regions tend to get wetter with rising temperatures (Fig. 3). Zones 9 and 10 (i.e. Boreal Plains and Canadian Prairies) maintain negative correlations throughout all seasons that reflect hot and dry

conditions prevalent in the region. More zones exhibit significant correlations in summer than in any other season, whereas the magnitude of the correlation is highest in spring and fall, reaching below -0.4 for the Prairies and the Boreal Plains, respectively. Correlations are negligible in winter with only the Boreal Plain exhibiting statistical significance.

Each copula is selected from a pool of candidate models according to the minimum AIC_c score and then evaluated using the goodness-of-fit test. Copulas selected for each season passed the goodness-of-fit test at a significance level of 5% with *p* values ranging from 0.44 in winter to 0.72 in spring providing strong evidence that the empirical data follow the selected parametric copula (*p* value = 1 indicates a perfect match). The dependence structure in the Boreal Plains is quite similar in all seasons except in summer (Fig. 4). The accumulated precipitation is highest in the summer with the peak copula density at a temperature of $13\text{ }^{\circ}\text{C}$ and $175\text{ mm season}^{-1}$ of rain. In all other seasons, the precipitation peak drops below $150\text{ mm season}^{-1}$ with the lowest amount in winter at under $100\text{ mm season}^{-1}$. In summer, the dependency between high temperature and low precipitation is evident in the lower tail indicating that hotter summers tend to receive lower than average precipitation. This corresponds to the prevalence of hot and dry conditions, which might exacerbate conditions that can lead to frequent droughts in the region. However, Stewart et al. (2012) showed that drought conditions are not only the result of hot and dry conditions but in fact, cold and dry conditions are common during droughts. They identified 15-month long cold-dry periods using the Standardized Precipitation Index, which occurred during droughts and mostly in late spring. The findings by Stewart et al. (2012)

Fig. 2 **a** and **b** Joe copula and R270 Clayton copula used to characterize the joint behaviour of temperature and precipitation in the southern Arctic and Prairies zones, respectively from 1950 to 2010. Red and grey points are the observed and simulated data overlaid with contour lines of the copula CDFs. The marginal distributions on the top (temperature-normal distribution) and on the right (precipitation–gamma distribution) follow the same colour scheme (red for observation and grey for copula simulations)



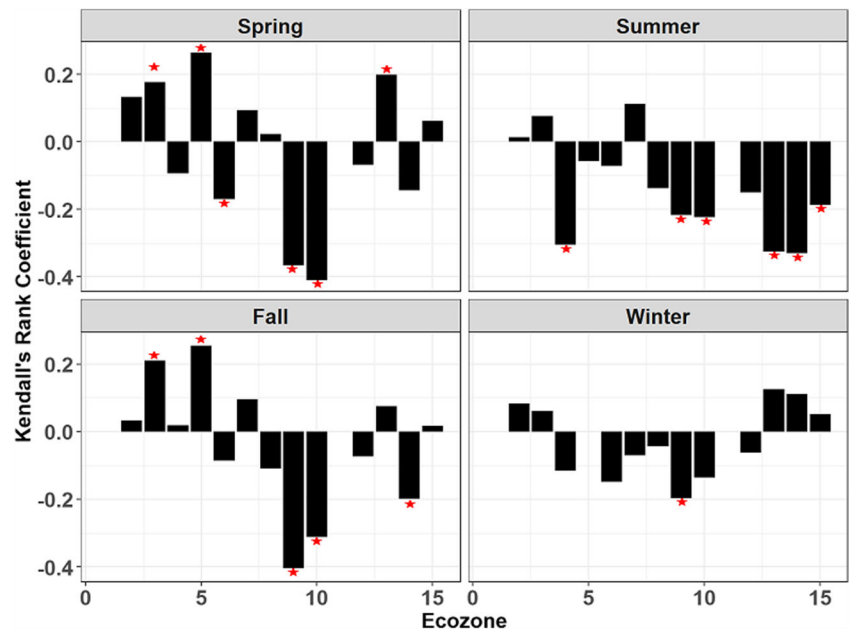
are reflected in this study with winter receiving the lowest amount of precipitation.

4.3 Monthly dependency

The northern and southern Arctic zones (Zones 2 and 3) show significantly strong positive correlations from October to March, whereas the Boreal Plains and Prairie zones (9 and 10) show significant negative

correlations throughout the year, peaking around the months of August to November (Fig. 5). In western zones, including the Pacific Maritime and Montane Cordillera, the dependence shifts from significantly positive in November to February to significantly negative in June to August and September. The majority of the copulas selected for these cases are the ones that exhibit both lower and upper tail dependence (2-parameter copulas) indicating correlation in extremes. Strong

Fig. 3 Kendall's rank coefficients across all zones in each season analyzed for 1950–2010. The red asterisk signifies statistically significant correlations at a level of 5%



concordance (i.e. positive dependence) in winter months suggests a wetting and warming trend, whereas the discordance in summer months hints towards hotter and drier conditions as temperatures rise. This is consistent with Merritt et al. (2006) who reported that winter temperatures are expected to rise by 1.5°–4.0 °C

with a corresponding 5–20% increase in precipitation by the 2050s. Zhang et al. (2000) reported similar findings with a significant increase in precipitation in all four seasons. They reported increases in snowfall due to increased winter precipitation, which can lead to larger deposits of snow and increases in the magnitude of late

Fig. 4 Copulas selected for the Boreal Plains zone in each season for 1950–2010 based on 9 stations in the zone. Circles and triangles represent copula simulations and observed data, respectively. The colour coding represents the joint quantiles of temperature and precipitation

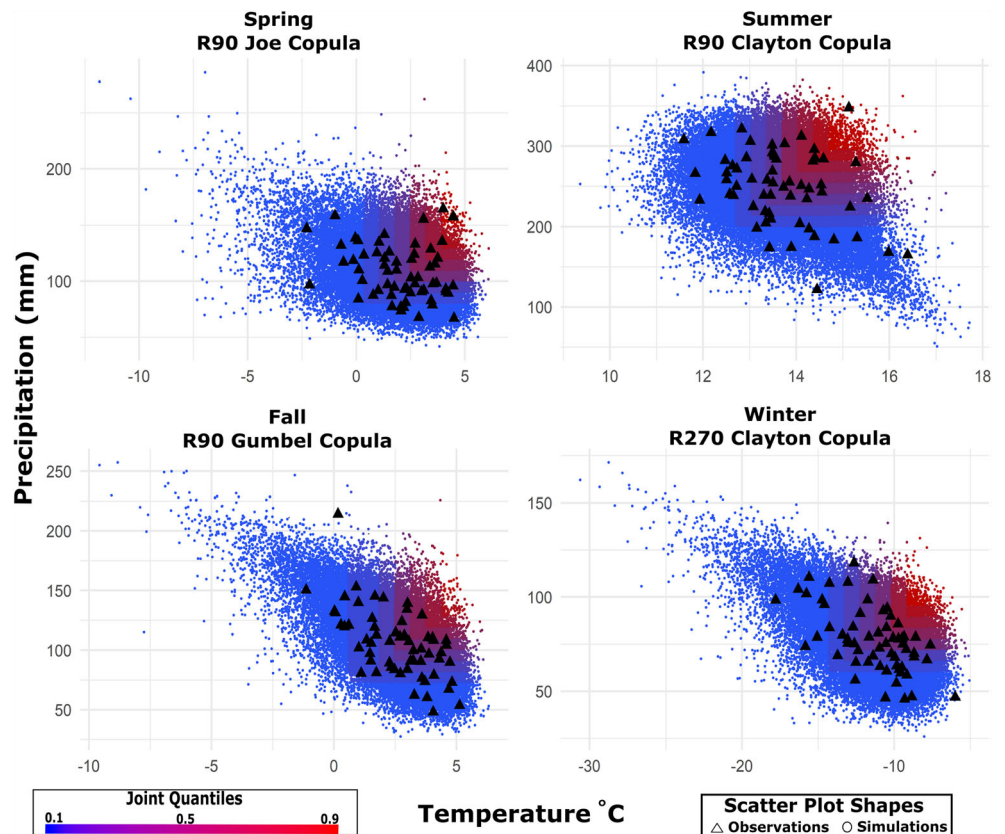
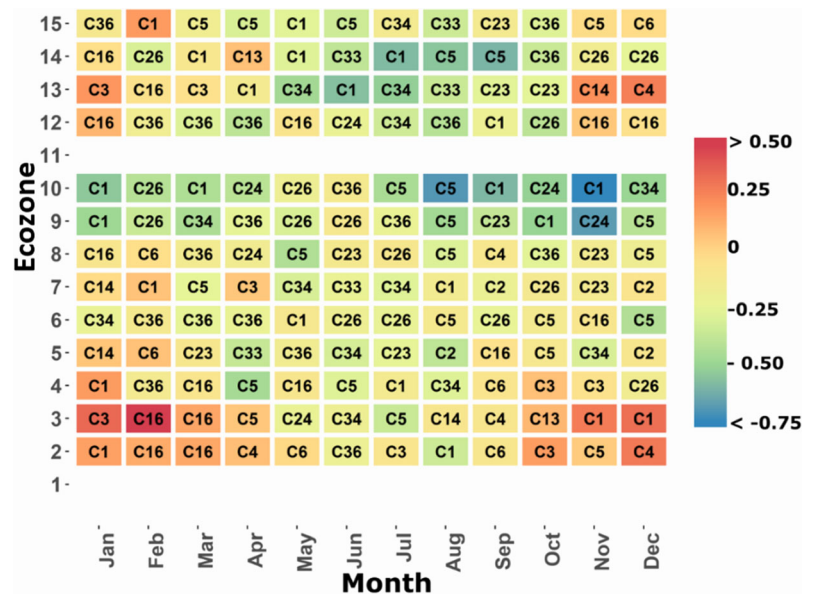


Fig. 5 Kendall’s rank correlation coefficient (colour scale) and the corresponding copula (symbol) selected for monthly aggregated data across all zones



winter–early spring flooding. This effect can be restricted to higher elevations as other studies have reported overall reductions in snow water equivalent in western Canada (Najafi et al. 2017b).

4.4 Non-stationary dependence structure

The Mann-Kendall trend test analysis is performed on the pre-whitened (if the significant serial correlation is found at a 5% significance level) temperature and precipitation data. Significant temperature trends are found in all zones except for Zone 14 (Montane Cordillera), whereas precipitation trends are statistically insignificant in all zones except for Zone 12 (Boreal Cordillera) (Table 4).

The non-stationary approach is applied at the seasonal time scale for each zone. The common observation among all zones and seasons is the warming trend over the last

century. Copula peak densities (i.e. the mode of the joint probability density function for each 50-year moving window) have shifted to the right on the temperature axis in every case while precipitation shows variations among zones and seasons. Here, we present the results of summer and winter seasons for the Mixed Wood Plains (Zone 8) and Boreal Plains (Zone 9). Results for other zones have been added in the supplementary material (Supplementary Figs. 1-6).

Figure 6 shows the peak of the joint distribution for each moving window, which depicts the most probable joint event within the corresponding time period. Results of Zone 8 (i.e. Mixed Wood Plains) show that the region has been getting warmer and wetter in the summer over the last century. Whereas temperature shows an approximate increase of 4% from the first to the last time window, precipitation shows an increase of almost 8% in the same period. In winter, temperature increases are higher

Table 4 *p* values of the Mann-Kendall trend test for temperature and precipitation. Values with asterisk symbol represent statistically significant trends at 5% significance level

Zone	Temperature trend (°C/108 years)	<i>P</i> value of temperature trend	Precipitation trend (mm/108 years)	<i>P</i> value of precipitation trend
6 – Boreal Shield	1.6	0.000*	4.9	0.055
7 – Atlantic Maritime	1.2	0.000*	5.8	0.066
8 – Mixedwood Plains	1.9	0.000*	5.3	0.118
9 – Boreal Plains	1.7	0.000*	0.6	0.398
10 – Prairies	1.9	0.001*	−1.2	0.740
12 – Boreal Cordillera	1.3	0.019*	8.2	0.019*
13 – Pacific Maritime	1.7	0.000*	4.0	0.275
14 – Montane Cordillera	0.9	0.445	0.9	0.056

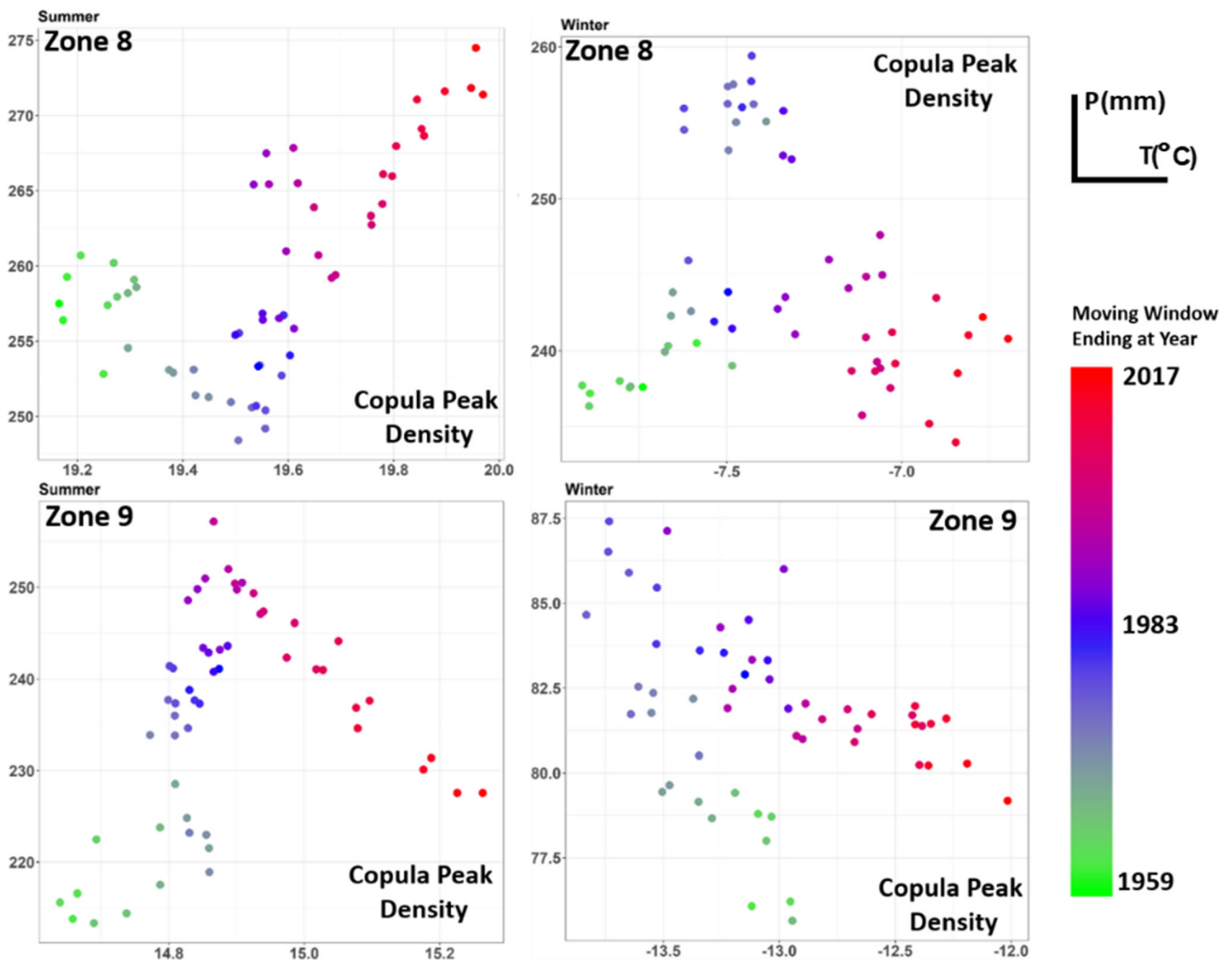


Fig. 6 Results of non-stationary copula analysis in Zone 8 (Mixed Wood Plains) and Zone 9 (Boreal Plains). The scatterplot shows the peak density (i.e. the most probable joint occurrence of temperature and precipitation)

at each 50-year moving window from 1900 to 1959 (the first window) to 1968–2017 (the last window). Precipitation is plotted along the Y-axis and temperature along the X-axis in each figure

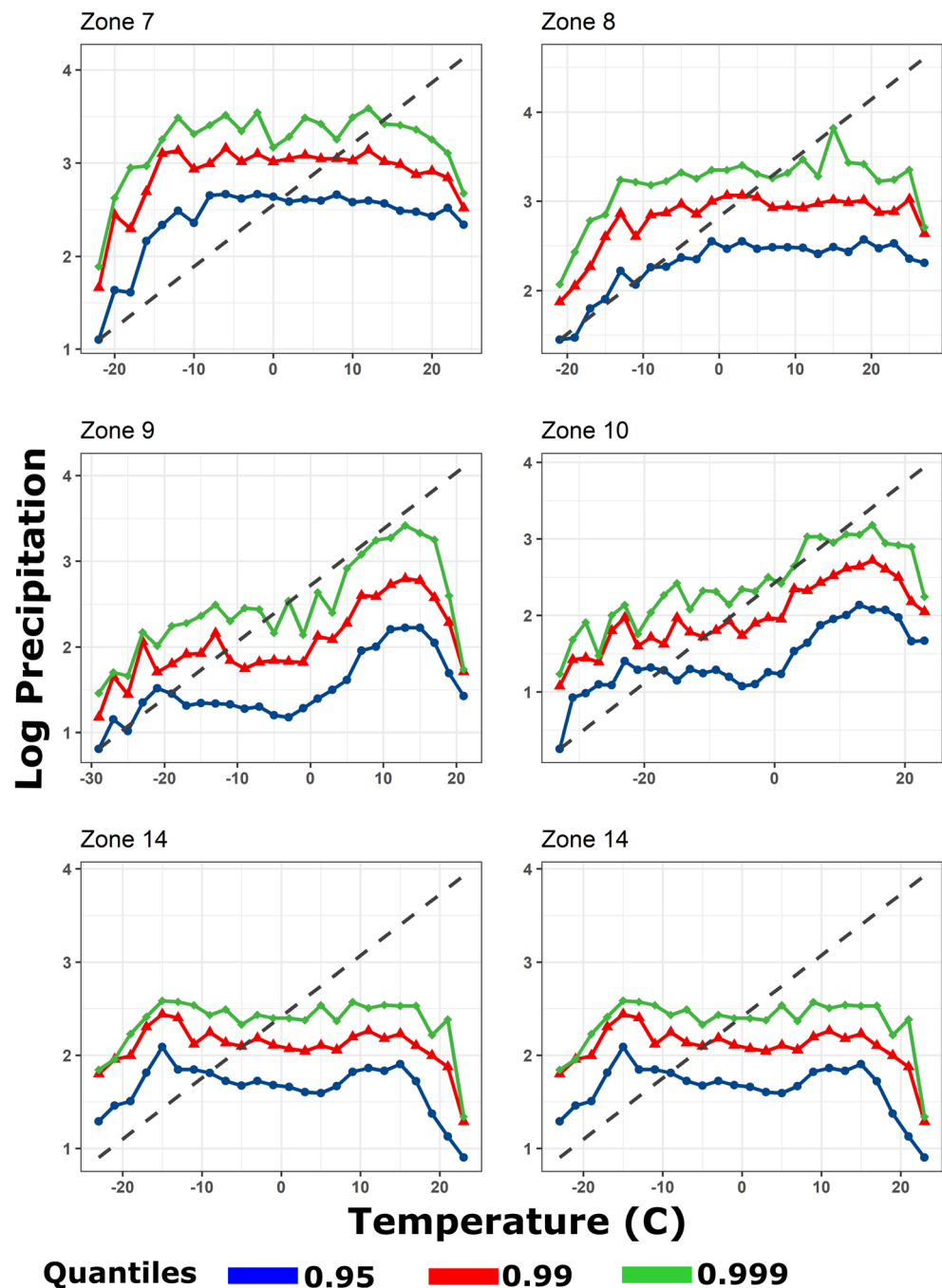
compared with the ones in the summer, close to 7%, but precipitation amounts show a step increase in the 1980s before returning to almost the same levels of the initial window by 2017. Although as discussed previously, Zone 8 does not show significant evidence of dependence between temperature and precipitation, the “warmer and wetter” trend in summer is in line with the joint behaviour observed in almost all other zones. The same was reported by Zhang et al. (2000) who observed that the joint 66th quantiles of temperature and precipitation have been growing larger in southern Canada indicating an increase in wetter and warmer conditions.

Zone 9 (i.e. Boreal Plain) shows a decline in precipitation levels with increasing temperatures in the latter half of the last century. This is similar to the findings of the seasonal analysis of the 1950–2010 period that showed a strong negative dependence between temperature and precipitation in all seasons particularly in summer.

4.5 CC scaling curves

The scaling rates of extreme precipitation mostly deviate from the theoretical value of $6.8\% \text{ } ^\circ\text{C}^{-1}$. Most regions show lower scaling rates (i.e. sub-CC) except in the north (Table 5). The scaling rates are also proportional to the precipitation amounts in almost all zones with the 95th quantile having the lowest scaling rates in every zone and the 99.9th quantile showing the highest rates (Fig. 7). This behaviour is consistent with the results obtained in previous studies (Hardwick Jones et al. 2010; Panthou et al. 2014; Singleton and Toumi 2013; Utsumi et al. 2011). One of the reasons that sub-CC scaling rates are observed is because precipitation is analyzed at a daily temporal scale while previous studies have shown that the CC scaling rates decline as the temporal scale increases from sub-daily to daily. For example, in a multi-time scale study over Quebec, Panthou et al. (2014) reported that as the temporal scale of precipitation increases from shorter to longer

Fig. 7 CC scaling curves for extreme precipitation and temperature. Grey dotted line corresponds to the theoretical scaling rate of $7.3\% \text{ } ^\circ\text{C}^{-1}$ at $0 \text{ } ^\circ\text{C}$. Blue, red and green lines represent the 95th, 99th and 99.9th quantiles of precipitation, respectively



durations, the CC scaling rate would decline. Hardwick Jones et al. (2010) provide another insight into the phenomenon that as the air temperature increases beyond $26 \text{ } ^\circ\text{C}$, there is a reduction in relative humidity in the air. They argue that even though the moisture-holding capacity of the air would theoretically increase with increasing temperature, the amount of moisture available to the air would decline at high temperatures thus causing a decline in extreme precipitation. Super-CC scaling rates (i.e. scaling rates over 6.8%) are observed in the northern regions consistent with Utsumi et al. (2011) who found increases in the global observed extreme precipitation

only at high latitudes ($> 55^\circ\text{N}$). To better understand the spatial variability of the scaling rates, a station by station analysis was also performed using similar procedure applied for each zone (Figs. S7-S9). The results show spatial heterogeneity of the scaling rates and sensitivity to the spatial scale. For example, one of the highest scaling rates (close to $+16\%$) is found at a site on the western coast but the scaling rate calculated over the zone in which that site lies is very low, showing the smoothing effect of other stations on extreme scaling rates of that particular site. The at-site CC ratios range between slightly negative rates (mostly in southwestern regions) to

Table 5 Scaling rates for extreme precipitation over Canadian ecozones

Quantile	Zone	Scaling (% ° C ⁻¹)	Zone	Scaling (% ° C ⁻¹)
95th	2	8.8	8	3.0
99th		11.0		3.2
99.9th		12.7		3.8
95th	3	7.6	9	2.6
99th		8.8		3.2
99.9th		10.0		3.7
95th	4	5.1	10	3.0
99th		6.1		3.7
99.9th		8.8		3.8
95th	5	3.0	13	-2.0
99th		3.4		0.2
99.9th		3.7		1.7
95th	6	1.6	14	0.8
99th		1.8		1.0
99.9th		2.8		1.6
95th	7	4.2	15	8.2
99th		4.6		8.3
99.9th		4.7		8.9

approximately + 16%. For each extreme quantile of precipitation, there were at least 30 stations with values more than the theoretical scaling rate indicating larger increases in extreme precipitation with rising temperature compared with CC estimates. For other stations, although the scaling ratio is below the theoretical value, they still point to increases in intense precipitation rates in a warmer climate.

5 Conclusion

This study characterizes the dependence structure between temperature and precipitation over Canada using copulas. The analyses are conducted over 15 terrestrial ecozones to represent the spatial patterns of the corresponding covariabilities at the annual, seasonal and monthly temporal scales. AHCCD station data are first spatially and then temporally aggregated within each ecozone of Canada to the respective timescales. The Kendall’s rank correlations are calculated and if significant correlations (at 5% significance level) are found, then the non-linear dependency is analyzed using copulas. Further, this procedure is adapted into a moving window copula analysis over long-term historical records dating back to 1910 to reveal the joint trends between temperature and precipitation. CC scaling curves are built for all zones to find evidence of changes in precipitation that might have occurred due to the gradual rise in temperature over the past decades.

The northern regions show relatively strong positive correlations between temperature and precipitation. In addition,

they show upper tail dependencies indicating that warmer periods tend to correlate with wetter periods in these regions. The Canadian Prairies, however, show strong negative dependencies between the two variables, with strong evidence of tail dependence between hot and dry conditions. The moving window analysis shows that while temperature trends are significant throughout southern Canada from 1910 to 2017, precipitation trends are spatially varied. Temperature increases are highest in the Boreal Plains and Prairies accompanied with negligible changes in precipitation in the Boreal Plains and a non-significant decrease in the Prairies. The consensus is that most regions tend to become warmer and wetter except for the zones in the Canadian Prairies, which show warmer and drier conditions. This is in line with the findings of stationary copulas. Southeastern Canada and zones around east and west of Hudson Bay show no significant dependencies between temperature and precipitation. In addition, extreme precipitation is studied with respect to temperature changes using the Clausius-Clapeyron scaling relationship. Large deviations from theoretical values are observed in all regions with super-CC scaling rates in the north and sub-CC scaling rates in most of the south, particularly the west coast where negative scaling rates were also observed. The study is limited by the number of observation records, especially in the northern regions of Canada. A potential future work would be extend this analysis to the whole spatial domain by incorporating data from reanalysis products and satellite based datasets.

This study shows the non-linear relationships exhibited by temperature and precipitation across Canada. The findings here can help better understand the effects of these two variables that result in compound scenarios such as the prevalence of warm-wet and hot-dry conditions.

Acknowledgements We thank Alex Cannon for his helpful comments on the observed data and model results.

Funding information Funding for this research is provided by Natural Sciences and Engineering Research Council of Canada (NSERC) Discovery Grant.

Appendix

CDF functions of some widely used copulas are provided in the following equations (Genest 1987; Joe 2014; Nelsen 2006). In all equations, u and v are the probability integral transforms of variables X and Y , θ and δ are the copula parameters and τ is the Kendall’s rank correlation coefficient between X and Y variables.

Clayton Copula:

$$C(u, v) = (u^{-\theta} + v^{-\theta} - 1)^{-\frac{1}{\theta}} \tag{9}$$

$$\tau = \theta / (\theta + 2) \tag{10}$$

Gumbel Copula:

$$C(u, v) = \exp\left(-\left[(-\log(u))^\theta + (-\log(v))^\theta\right]^{1/\theta}\right) \tag{11}$$

$$\tau = 1 - \theta^{-1} \tag{12}$$

Joe Copula:

$$C(u, v) = 1 - \left([1-u]^\theta + [1-v]^\theta - [1-u]^\theta [1-v]^\theta\right)^{1/\theta} \tag{13}$$

$$\tau = 1 + 2(2-\theta)^{-1} [\text{digamma}(2) - \text{digamma}(2/\theta + 1)] \tag{14}$$

Frank Copula:

$$C(u, v) = -\theta^{-1} \log\left(1 + \frac{(e^{-\theta u} - 1)(e^{-\theta v} - 1)}{(e^{-\theta} - 1)}\right) \tag{15}$$

$$\tau = 1 + 4\theta^{-1} [D_1(\theta) - 1] \tag{16}$$

$$D_k(x) = kx^{-k} \int_0^x t^{k-1} (e^t - 1)^{-1} dt \tag{17}$$

BB1 Copula:

$$C(u, v) = \left(1 + \left[(u^{-\theta} - 1)^\delta + (v^{-\theta} - 1)^\delta\right]^{1/\delta}\right)^{1/\theta} \tag{18}$$

$$\tau = 1 - 2 / [\delta(\theta + 2)] \tag{19}$$

BB6 Copula:

$$C(u, v) = 1 - \left(1 - \exp\left\{-\left[(-\log(1-u^{-\theta}))^\delta + (-\log(1-v^{-\theta}))^\delta\right]^{1/\delta}\right\}\right)^{1/\theta} \tag{20}$$

BB7 Copula:

$$C(u, v) = 1 - \left(1 - \left[(1-u^{-\theta})^{-\delta} (1-v^{-\theta})^{-\delta} - 1\right]^{-1/\delta}\right)^{1/\theta} \tag{21}$$

BB8 Copula:

$$C(u, v) = \frac{1 - \left(1 - \omega^{-1} \left[1 - (1 - \delta u)^\theta\right] \left[1 - (1 - \delta v)^\theta\right]\right)^{1/\theta}}{\delta} \tag{22}$$

$$\omega = 1 - (1 - \delta)^\theta \tag{23}$$

The densities of the rotated copulas are defined as:
Rotated-90 copula:

$$C^{90}(u, v) = C(1-u, v) \tag{24}$$

Rotated-180 copula or Survival Copula:

$$C^{180}(u, v) = C(1-u, 1-v) \tag{25}$$

Rotated-270 copula:

$$C^{270}(u, v) = C(v, 1-u) \tag{26}$$

References

Akaike H (1974) A new look at the statistical model identification. In: Parzen E, Tanabe K, Kitagawa G (eds) Selected Papers of Hirotugu Akaike. Springer Series in Statistics (Perspectives in Statistics), vol 19 (6). Springer, New York, pp 215–222. https://doi.org/10.1007/978-1-4612-1694-0_16

Allen CD et al (2010) A global overview of drought and heat-induced tree mortality reveals emerging climate change risks for forests. *For Ecol Manag* 259.4:660–684. <https://doi.org/10.1016/j.foreco.2009.09.001>

Anderson TW (1962) An introduction to multivariate statistical analysis (No. 519.9 A53). Wiley, New York

Anderson DR, Burnham K (2004) Model selection and multi-model inference. Second. Springer-Verlag, New York, p 63

Asong ZE, Khaliq MN, Wheater HS (2016) Multisite multivariate modeling of daily precipitation and temperature in the Canadian Prairie Provinces using generalized linear models. *Clim Dyn* 47:2901–2921. <https://doi.org/10.1007/s00382-016-3004-z>

Bender J, Wahl T, Jensen J (2014) Multivariate design in the presence of non-stationarity. *J HYDROL* 6(514):123–130. <https://doi.org/10.1016/j.jhydrol.2014.04.017>

Beniston M (2009) Trends in joint quantiles of temperature and precipitation in Europe since 1901 and projected for 2100. *Geophys Res Lett* 36:L07707. <https://doi.org/10.1029/2008GL037119>

Bintanja R, Selten FM (2014) Future increases in Arctic precipitation linked to local evaporation and sea-ice retreat. *Nature*. 2104 May 509(7501):479. <https://doi.org/10.1038/nature13259>

Bird PM, Rapport D (1986) State of the environment report for Canada. Environment, Canada

Burnham KP, Anderson DR, Huyvaert KP (2011) AIC model selection and multimodel inference in behavioral ecology: some background, observations, and comparisons. *Behav Ecol Sociobiol* 65:23–35. <https://doi.org/10.1007/s00265-010-1029-6>

Bush E, Lemmen DS (2019) Canada’s changing climate report; Government of Canada, Ottawa, ON pp 444

Cong R, Brady M (2012) The interdependence between rainfall and temperature: copula analyses. *Sci World J* 2012:405675, 11 pages. <https://doi.org/10.1100/2012/405675>

Déry SJ, Wood EF (2005) Observed twentieth century land surface air temperature and precipitation covariability. *Geophys Res Lett* 32: L21414. <https://doi.org/10.1029/2005GL024234>

Directorate L (1986) Lands Directorate, Terrestrial Ecozones Of Canada, Ecological Land Classification No. 19, p. 26

Environment Canada (2014). Canada’s Sixth National Report on Climate Change

Favre AC, El Adlouni S, Perreault L, Thiémond N, Bobée B (2004) Multivariate hydrological frequency analysis using copulas, *water Resour. Res.* 40:W01101. <https://doi.org/10.1029/2003WR002456>

Frees EW, Valdez EA (1998) Understanding relationships using copulas. *N. AM. ACTUAR. J* 2(1):1–25. <https://doi.org/10.1080/10920277.1998.10595667>

Genest C (1987) Frank’s family of bivariate distributions. *Biometrika* 74(3):549–555. <https://doi.org/10.1093/biomet/74.3.549>

- Genest C, Favre AC (2007) Everything you always wanted to know about copula modeling but were afraid to ask. *J Hydrol Eng* 12(4):347–368. [https://doi.org/10.1061/\(ASCE\)1084-0699\(2007\)12:4\(347\)](https://doi.org/10.1061/(ASCE)1084-0699(2007)12:4(347))
- Genest C, Rémillard B (2008) Validity of the parametric bootstrap for goodness-of-fit testing in semiparametric models. *ANN I H POINCARÉ-PR* 44(6):1096–1127. <https://doi.org/10.1214/07-AIHP148>
- Genest C, Rivest LP (1993) Statistical inference procedures for bivariate Archimedean copulas. *J Am Stat Assoc* 88(423):1034–1043. <https://doi.org/10.1080/01621459.1993.10476372>
- GENEST C, QUESSY J, RÉMILLARD B (2006) Goodness-of-fit procedures for copula models based on the probability integral transformation. *Scand J Stat* 33:337–366. <https://doi.org/10.1111/j.1467-9469.2006.00470.x>
- Gennaretti F, Sangelantoni L, Grenier P (2015) Toward daily climate scenarios for Canadian Arctic coastal zones with more realistic temperature-precipitation interdependence. *J Geophys Res Atmos* 120:11,862–11,877. <https://doi.org/10.1002/2015JD023890>
- Guerfi N, Assani AA, Mesfioui M, Kinnard C (2015) Comparison of the temporal variability of winter daily extreme temperatures and precipitations in southern Quebec (Canada) using the Lombard and copula methods. *Int J Climatol* 35:4237–4246. <https://doi.org/10.1002/joc.4282>
- Hao Z, Singh VP (2016) Review of dependence modeling in hydrology and water resources. *Prog Phys Geogr* 40(4):549–578. <https://doi.org/10.1177/0309133316632460>
- Hardwick JR, Westra S, Sharma A (2010) Observed relationships between extreme sub-daily precipitation, surface temperature, and relative humidity. *Geophys Res Lett* 37(22). <https://doi.org/10.1029/2010GL045081>
- Henze N (1996) Empirical-distribution-function goodness-of-fit tests for discrete models. *Can J Stat* 24:81–93. <https://doi.org/10.2307/3315691>
- Isaac GA, Stuart RA (1992) Temperature–precipitation relationships for Canadian stations. *J Clim* 5(8):822–830. [https://doi.org/10.1175/1520-0442\(1992\)005%3C0822:TRFCS%3E2.0.CO;2](https://doi.org/10.1175/1520-0442(1992)005%3C0822:TRFCS%3E2.0.CO;2)
- Joe H (2014) Dependence modeling with copulas, 1st ed, p 480. Chapman and Hall/CRC, New York. <https://doi.org/10.1201/b17116>
- Johnson RA, Wichern DW (2002) Applied multivariate statistical analysis, vol 5. Prentice hall, Upper Saddle River
- Laux P, Vogl S, Qiu W, Knoche HR, Kunstmann H (2011) Copula-based statistical refinement of precipitation in RCM simulations over complex terrain. *Hydrol Earth Syst Sci* 15(7):2401–2419
- Lazoglou G, Anagnostopoulou C (2019) Joint distribution of temperature and precipitation in the Mediterranean, using the copula method. *Theor Appl Climatol* 135(3–4):1399–1411. <https://doi.org/10.1007/s00704-018-2447-z>
- Mekis E, Vincent LA (2011) An overview of the second generation adjusted daily precipitation dataset for trend analysis in Canada. *Atmosphere-Ocean* 49(2):163–177. <https://doi.org/10.1080/07055900.2011.583910>
- Merritt WS, Alila Y, Barton M, Taylor B, Cohen S, Neilsen D (2006) Hydrologic response to scenarios of climate change in sub watersheds of the Okanagan basin, British Columbia. *J Hydrol* 326(1–4): 79–108. <https://doi.org/10.1016/j.jhydrol.2005.10.025>
- Najafi MR, Zwiers FW, Gillett NP (2016) Attribution of the spring snow cover extent decline in the Northern Hemisphere, Eurasia and North America to anthropogenic influence. *Clim Chang* 136(3–4):571–586. <https://doi.org/10.1007/s10584-016-1632-2>
- Najafi MR, Zwiers FW, Gillett NP (2017a) Attribution of observed streamflow changes in key British Columbia drainage basins. *Geophys Res Lett* 44:11,012–11,020. <https://doi.org/10.1002/2017GL075016>
- Najafi MR, Zwiers F, Gillett N (2017b) Attribution of the observed spring snowpack decline in British Columbia to anthropogenic climate change. *J Clim* 30(11):4113–4130. <https://doi.org/10.1175/JCLI-D-16-0189.1>
- Nelsen RB (2006) An introduction to copulas, 2nd ed, p XIV, 272. Springer-Verlag, New York. <https://doi.org/10.1007/0-387-28678-0>
- Pall P, Allen MR, Stone DA (2007) Testing the Clausius–Clapeyron constraint on changes in extreme precipitation under CO₂ warming. *Clim Dyn* 28(4):351–363. <https://doi.org/10.1007/s00382-006-0180-2>
- Panthou G, Mailhot A, Laurence E, Talbot G (2014) Relationship between surface temperature and extreme rainfalls: a multi-time-scale and event-based analysis. *J Hydrometeorol* 15(5):1999–2011. <https://doi.org/10.1175/JHM-D-14-0020.1>
- Peel MC, Finlayson BL, TA MM (2007) Updated world map of the Köppen–Geiger climate classification. *Hydrol Earth Syst Sci* 11: 1633–1644
- Rana A, Moradkhani H, Qin Y (2017) Understanding the joint behavior of temperature and precipitation for climate change impact studies. *Theor Appl Climatol* 129(1–2):321–339. <https://doi.org/10.1007/s00704-016-1774-1>
- Salvadori G, De Michele C (2004) Frequency analysis via copulas: theoretical aspects and applications to hydrological events, water resour. Res. 40:W12511. <https://doi.org/10.1029/2004WR003133>
- Schepsmeier U et al (2018) VineCopula: statistical inference of vine copulas. R package version 2(1):8
- Schmidt T (2007) Coping with copulas. copulas - from theory to applications in finance:3–34
- Schoelzel C, Friederichs P (2008) Multivariate non-normally distributed random variables in climate research—introduction to the copula approach. *Nonlinear Process Geophys* 15(5):761–772
- Shiau JT (2006) Fitting drought duration and severity with two-dimensional copulas. *Water Resour Manag* 20(5):795–815. <https://doi.org/10.1007/s11269-005-9008-9>
- Singleton A, Toumi R (2013) Super-Clausius–Clapeyron scaling of rainfall in a model squall line. *QJRMAM* 139:334–339. <https://doi.org/10.1002/qj.1919>
- Sklar M (1959) Fonctions de repartition an dimensions et leurs marges. *Publ inst statist univ Paris* 8:229–231
- Stewart RE, Bonsal BR, Harder P, Henson W, Kochtubajda B (2012) Cold and hot periods associated with dry conditions over the Canadian prairies. *Atmosphere-Ocean* 50(3):364–372. <https://doi.org/10.1080/07055900.2012.673164>
- Stute W, Manteiga WG, Quindimil MP (1993) Bootstrap based goodness-of-fit-tests. *Metrika* 40(1):243–256. <https://doi.org/10.1007/BF02613687>
- Tencer B, Weaver A, Zwiers F (2014) Joint occurrence of daily temperature and precipitation extreme events over Canada. *J Appl Meteorol Climatol* 53(9):2148–2162. <https://doi.org/10.1175/JAMC-D-13-0361.1>
- Trenberth KE, Shea DJ (2005) Relationships between precipitation and surface temperature. *Geophys Res Lett* 32:L14703. <https://doi.org/10.1029/2005GL022760>
- Utsumi N, Seto S, Kanae S, Maeda EE, Oki T (2011) Does higher surface temperature intensify extreme precipitation? *Geophys Res Lett* 38: L16708. <https://doi.org/10.1029/2011GL048426>
- Vincent LA, Wang XL, Milewska EJ, Wan H, Yang F, Swail V (2012) A second generation of homogenized Canadian monthly surface air temperature for climate trend analysis. *J Geophys Res* 117: D18110. <https://doi.org/10.1029/2012JD017859>
- Vincent LA et al (2015) Observed trends in Canada’s climate and influence of low-frequency variability modes. *J Clim* 28(11):4545–4560. <https://doi.org/10.1175/JCLI-D-14-00697.1>
- Vincent LA, Zhang X, Mekis É, Wan H, Bush EJ (2018) Changes in Canada’s climate: trends in indices based on daily temperature and precipitation data. *Atmosphere-Ocean* 56(5):332–349. <https://doi.org/10.1080/07055900.2018.1514579>

- Wang W, Wells MT (2000) Model selection and semiparametric inference for bivariate failure-time data. *J Am Stat Assoc* 95(449):62–72. <https://doi.org/10.1080/01621459.2000.10473899>
- Wiken EB (1986) Terrestrial ecozones of Canada, ecological land classification series no. 19. Environment Canada, Ottawa
- Wong G, Lambert MF, Leonard M, Metcalfe AV (2009) Drought analysis using trivariate copulas conditional on climatic states. *J Hydrol Eng* 15(2):129–141. [https://doi.org/10.1061/\(ASCE\)HE.1943-5584.0000169](https://doi.org/10.1061/(ASCE)HE.1943-5584.0000169)
- Zhang LS, Singh VP (2006) Bivariate flood frequency analysis using the copula method. *J Hydrol Eng* 11(2):150–164. [https://doi.org/10.1061/\(ASCE\)1084-0699\(2006\)11:2\(150\)](https://doi.org/10.1061/(ASCE)1084-0699(2006)11:2(150))
- Zhang X, Vincent LA, Hogg WD, Niitsoo A (2000) Temperature and precipitation trends in Canada during the 20th century. *Atmosphere-ocean* 38(3):395–429. <https://doi.org/10.1080/07055900.2000.9649654>
- Zwiers FW, Von Storch H (1995) Taking serial correlation into account in tests of the mean. *J Clim* 8(2):336–351. [https://doi.org/10.1175/1520-0442\(1995\)008<0336:TSCIAI>2.0.CO;2](https://doi.org/10.1175/1520-0442(1995)008<0336:TSCIAI>2.0.CO;2)

Publisher's note Springer Nature remains neutral with regard to jurisdictional claims in published maps and institutional affiliations.